Rotational State Microwave Mixing for Laser Cooling of Complex Diatomic Molecules

Mark Yeo, Matthew T. Hummon, Alejandra L. Collopy, Bo Yan, Boerge Hemmerling, Eunmi Chae, John M. Doyle, and Jun Ye

Phys. Rev. Lett. **114**, 223003 — Published 5 June 2015

DOI: 10.1103/PhysRevLett.114.223003

Rotational state microwave mixing for laser cooling of complex diatomic molecules

Mark Yeo,[1,*] Matthew T. Hummon,[1] Alejandra L. Collopy,[1] Bo Yan,[1]
Boerge Hemmerling,[2,3] Eunmi Chae,[2,3] John M. Doyle,[2,3] and Jun Ye[1]

[1] *JILA, National Institute of Standards and Technology and University of Colorado, and Department of Physics, University of Colorado, Boulder, CO 80309*
[2] *Department of Physics, Harvard University, Cambridge, MA 02138, USA*
[3] *Harvard-MIT Center for Ultracold Atoms, Cambridge, MA 02138, USA*

We demonstrate the mixing of rotational states in the ground electronic state using microwave radiation to enhance optical cycling in the molecule yttrium (II) monoxide (YO). This mixing technique is used in conjunction with a frequency modulated and chirped continuous wave laser to slow longitudinally a cryogenic buffer gas beam of YO. We generate a flux of YO below 10 m/s, directly loadable into a three-dimensional magneto-optical trap. This technique opens the door for laser cooling of diatomic molecules with more complex loss channels due to intermediate states.

PACS numbers: 37.10.Mn, 37.10.Pq, 37.10.Vz

The field of cold and ultracold molecules is undergoing rapid growth with the development of new techniques and applications [1]. Cold polar molecules are continuing to improve tests of fundamental symmetries [2–6]. The strong dipolar interaction present in polar molecules also yields a rich set of applications in novel quantum matter [7–9] and cold chemistry [10–12].

A slow molecular source is often desirable in these applications to either enhance interaction time or for trap loading. The magneto-association and coherent state transfer of ultracold alkali atoms [13] can produce polar molecules near quantum degeneracy. Supersonic beams produce molecules with forward velocity $\gtrsim 300$ m/s [14], whereas cryogenic buffer gas beams have velocities of 50-200 m/s, depending on source configuration [15] and with the lower velocity beams directly loadable into a trap [16]. Many techniques to further slow these beams have been developed. Stark [17, 18] and Zeeman [19, 20] deceleration have been used to load conservative traps, which can be used for evaporation [21]. Centrifugal slowing [22] and opto-electric cooling was demonstrated with CH_3F molecules [23]. The rovibrational branching that prevents optical cycling transitions in molecules was addressed theoretically [24, 25] and optical Doppler cooling was subsequently demonstrated in the SrF system [26]. Magneto-optical trapping was proposed for TiO [25] and demonstrated in two dimensions for YO [27] and in three dimensions for SrF [28, 29].

While directly loading a buffer-gas cooled atomic beam into a three-dimensional (3D) magneto-optic trap (MOT) is possible [30], for molecules with much lower photon scattering rates longitudinal optical cooling is necessary for loading into a 3D MOT. Typically 10^4 photons must be scattered to slow molecules to within the capture velocities of a MOT. During the slowing process, the molecular transition used for optical cooling experiences a Doppler frequency shift of tens or hundreds of resonance linewidths, resulting in inefficient photon scattering for a monochromatic unchirped laser beam. To date, molecules that have been laser cooled all have the magnetic sub-levels in the ground electronic state continually remixed by the multi-leveled optical cycling process. Hence, the widely used atomic Zeeman slower [31], which relies on the Zeeman shift of a single magnetic sublevel to compensate for the Doppler shift during deceleration is not applicable. To maintain a sufficiently large optical scattering rate throughout the slowing process, two techniques have been employed. Chirping the laser frequency was shown to reduce the velocity of a supersonic beam of CaF by 30 m/s [32]. For SrF, broadband laser radiation was used to slow molecules to be loaded directly into a 3D MOT [28].

Optical cycling in molecules [25, 26] is critical for the radiation pressure force to directly slow and cool molecular beams. However, achieving optical cycling in a large class of molecules remains difficult due to optical pumping into dark states. While vibrational dark states can be addressed with repump lasers [24], rotational dark states often have parity selection rules that prevent direct optical repumping. There are several loss mechanisms that break the rotational closure in current molecular optical cycling schemes, and they arise from additional decays via intermediate states or higher order transition moments. Vibrational states have lifetimes $\sim$1 s [33], and rovibrational decay is not yet a limiting factor for current techniques. Decays via magnetic dipole transitions are typically suppressed by a factor of $\alpha^2 \approx 5\times10^{-5}$ compared to electric dipole transitions (α is the fine structure constant), though recent measurements in OH indicate that they can be a factor of 10 faster than expected [34]. For some molecules, maintaining optical cycling can be more complex due to decays through intermediate electronic states, present in, for example, YO [35] and BaF [36]. Such decays are normally suppressed by the relatively long transition wavelengths. For YO the suppression factor is $\sim 3 \times 10^{-4}$. However, the decay is sufficient to cause population leakage to rotational dark states when a large number of photon scattering is needed

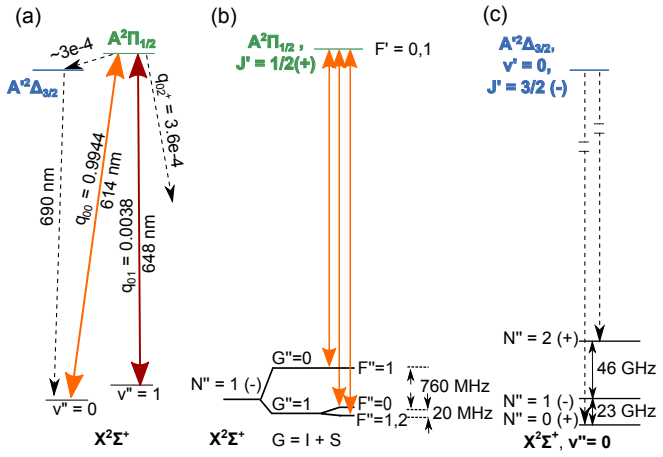

FIG. 1. (Color online) (a) YO vibronic structure. Dashed arrows indicate decay paths with corresponding Franck-Condon factors, q [37]. Solid arrows indicate cooling and repump laser transitions. (b) Hyperfine structure. Solid arrows indicate the three hyperfine pumping components used in each vibrational manifold. (c) Rotational mixing. Dashed arrows indicate the decay paths to $X^2\Sigma$ through the $A'^2\Delta_{3/2}$ state and black solid arrows show the microwave rotational mixing.

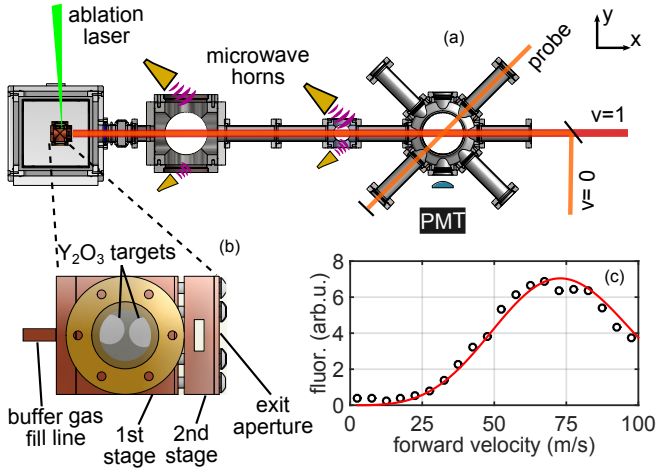

FIG. 2. (Color online) (a) Depiction of the beam apparatus. The YO molecular beam interacts with a counter-propagating slowing laser beam along x. A 45° probe beam is used for Doppler sensitive detection. A PMT is used to collect fluorescence induced by either the slowing or probe beam. (b) Two-stage buffer gas cell. (c) Velocity distribution measured at the detection region. The solid line is a fit to a Gaussian (with center longitudinal velocity of the beam at 49 m/s and a temperature of 8 K) multiplied by the square of the forward velocity to account for the transverse velocity spread.

for cooling. In this Letter, we report microwave mixing of rotational states to close these additional loss channels. This enables us to slow longitudinally a beam of YO emitting from a two-stage buffer gas cell to molecular velocities < 10 m/s, which can be loaded into a 3D MOT.

The optical cycling transition in YO proceeds between the $X^2\Sigma \rightarrow A^2\Pi_{1/2}$ states as described in Ref. [27]. In brief, highly diagonal Franck-Condon factors limit vibrational branching [37] such that a single repump laser limits its branching loss to 3.6×10^{-4} (Fig. 1(a)). Rotational branching is suppressed by a combination of parity and angular momentum selection rules [25, 38] when driving the $X^2\Sigma, N'' = 1$ level, where N is the rotation quantum number. Figure 1(b) shows the hyperfine structure of the $X^2\Sigma$ states, where G is the coupled nuclear and electronic spin, and F is the total angular momentum. For the $A^2\Pi_{1/2}$ and $A'^2\Delta_{3/2}$ states, J is the total angular momentum excluding nuclear spin. For all electronic states, $p = \pm$ represents the parity.

Figure 1(a) shows the additional loss channel where the $A^2\Pi_{1/2}$, $J' = 1/2$ state decays to the $A'^2\Delta_{3/2}$, $J' = 3/2$ state. Decays to states of higher J are forbidden due to angular momentum selection rules. The $A'^2\Delta_{3/2}$ state has a radiative lifetime of $\sim$1 μs [35] and will rapidly decay back to the $X^2\Sigma$ state. Since the full cycle starting from and returning to the ground state is a three-photon process, parity selection rules allow decays only to even rotational states (Fig. 1(c)). In the $X^2\Sigma$ state, while J is not a good quantum number, each rotational state can be expressed in terms of states with $J'' = N'' \pm 1/2$. The $\Delta J = 0, \pm 1$ angular momentum selection rule prevents decay to $N'' \geq 4$ ($J'' \geq 7/2$) and leads to optical pumping into the $N'' = 0, 2$ states. The rotational constant, B, for the $X^2\Sigma$ state is 11.634 GHz. Microwave radiation tuned to $2B$ ($4B$) can mix the $N'' = 0$ (2) levels with the $N'' = 1$ level. This mixing effectively removes the rotational dark states; however the maximum optical scattering rate is lowered as the number of states in $X^2\Sigma$ involved in optical cycling increases by a factor of two.

We employ this rotational state microwave mixing scheme for longitudinal slowing of a YO beam generated from a cryogenic buffer gas beam source. We laser ablate sintered Y_2O_3 pellets in a copper cell filled with helium buffer gas at 3.5 K (Fig. 2(a)). The hot YO thermalizes rotationally and translationally to the cold helium and the two stage cell [15] produces a YO beam with forward velocity of 70 m/s. The YO beam then travels 89 cm to the detection region, during which it may be illuminated by a 6 mm diameter, counter-propagating slowing beam. The 614 nm $v'' = 0$ laser has 70 mW of power and the 648 nm $v'' = 1$ laser has 80 mW (Fig. 1(a)). The slowing laser has three frequency components to address the hyperfine manifold (Fig. 1(b)). To provide the rotational mixing, we use two pairs of microwave horns located along the beam path, each pair producing $\sim$1 mW of either the 23 GHz or 46 GHz microwaves.

For velocity sensitive detection, we measure the fluorescence induced by a low intensity 4 mW/cm^2, 614 nm beam aligned 45° to the molecular beam. This probe

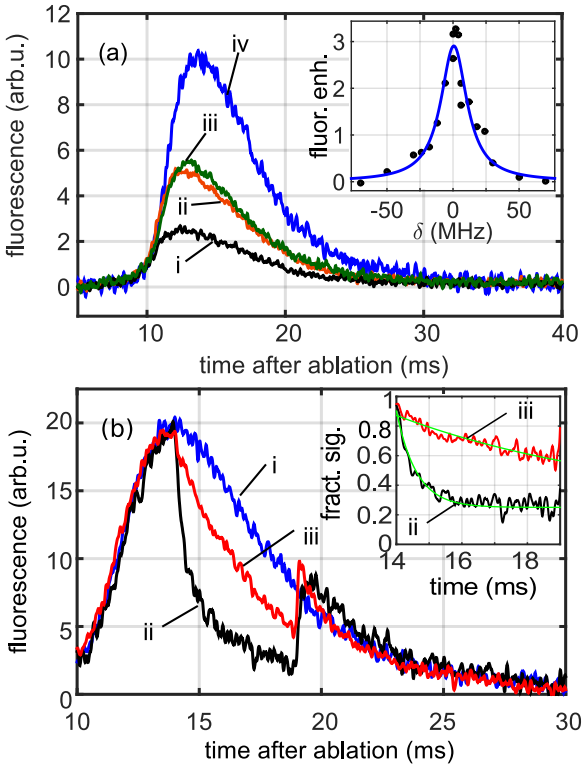

FIG. 3. (Color online) (a) Optical cycling enhancement due to rotational mixing. The fluorescence is induced by the high power optical slowing beam and $v'' = 1$ repump: (i) No mixing; (ii) $N'' = 0 \leftrightarrow N'' = 1$ mixing only; (iii) $N'' = 2 \leftrightarrow N'' = 1$ mixing only; (iv) simultaneous $N'' = 2 \leftrightarrow N'' = 1$ and $N'' = 0 \leftrightarrow N'' = 1$ mixing. The inset shows the fractional enhancement of optical scattering vs. microwave detuning from the rotational resonance. (b) Comparison of branching losses between $v'' = 1$ and $A'^2\Delta_{3/2}$: (i) Microwaves and $v'' = 0, 1$ are on throughout; (ii) $v'' = 1$ repump is shut off from 14-19 ms after ablation; (iii) Microwave mixing is switched off from 14-19 ms. The inset shows curves (ii) and (iii) divided by curve (i). Solid green lines are exponential fits.

laser has a saturation parameter of ∼0.5 and two frequency components separated by 780 MHz (Fig. 1(b)). This eliminates mechanical and optical pumping effects from the detection beam. The detection laser can be scanned over a range of ∼100 MHz at a rate of 1 kHz, corresponding to a velocity detection range of ∼100 m/s.

We study the rotational mixing by observing the fluorescence induced by the slowing beam in Fig. 3(a). We apply the microwaves in four binary combinations. For case i, no microwaves are applied. In contrast, when microwave mixing is applied to both $N'' = 0, 2$, (curve iv), there is a factor of four increase in fluorescence. Applying only the $N'' = 0 \leftrightarrow N'' = 1$ or $N'' = 2 \leftrightarrow N'' = 1$ mixing (Fig. 3(b) ii, iii respectively), we see a factor of two increase in fluorescence compared to case i. We estimate the vibrational lifetime of the $v'' = 1$ state from molecular parameters calculated in Ref. [39] to be ∼600 ms, much longer than the optical pumping time scale. The branching ratios for magnetic dipole transitions from the $A^2\Pi_{1/2}$ state is 2/3(1/3) for the $N'' = 0(2)$ levels in the $X^2\Sigma$ state, while electric dipole transitions from the $A'^2\Delta_{3/2}$ state have equal branching ratios to the $N'' = 0, 2$ rotational levels, consistent with curves ii and iii. Hence, decays through the intermediate $A'^2\Delta_{3/2}$ state are identified to be the dominant process.

To verify that the mixing microwaves are sufficiently strong to address all hyperfine states without the need of additional frequency sidebands, we simultaneously vary the frequency of the $N'' = 1 \leftrightarrow N'' = 0(2)$ mixing microwave by $\delta(2\delta)$ and measure the corresponding enhancement in fluorescence (Fig. 3(a) inset). This enhancement follows a 24 MHz full-width half-maximum Lorentzian lineshape, larger than the hyperfine variations of <5 MHz among the three relevant rotational manifolds [40, 41]. The mixing for higher vibrational states is suppressed because the rotational constant B for $v'' = 1$ is 50 MHz smaller than that for $v'' = 0$. This results in a 100 (200) MHz detuning for the $N'' = 0$ (2) transition in $v'' = 1$. Hence, we do not suffer any further reduction in the maximum optical cycling rate.

In Fig. 3(b), we study the time dependence of the optical pumping into $v'' = 1$, and also into rotational dark states via a previously unexplored branching route from the $A^2\Pi_{1/2}$ state to the $A'^2\Delta_{3/2}$ state. Again we measure the fluorescence induced by the slowing beam. For case i, the slowing and repumping light as well as microwaves are turned on at all times. For case ii, the $v'' = 1$ repump laser is rapidly shut off in ∼10 μs from 14 ms to 19 ms after ablation. This leads to an abrupt decrease in the fluorescence as the YO molecules are rapidly pumped into the $v'' = 1$ state and turn dark. To extract this pumping rate, we divide curve (ii) by curve (i) and fit an exponential with a constant background ratio of 0.25, resulting in a $1/e$ time constant of 620 μs. Combining this with the calculated Franck-Condon factor $q_{01} = 3.8 \times 10^{-3}$ [37], yields a photon scattering rate of 4.3×10^5 s^{-1}. This is smaller than the maximum possible scattering rate by a factor of ∼5 [27] and may be due to inefficient depletion due to highly Doppler detuned molecules, insufficient power in the wings of the slowing beam or an overestimate of the q_{01} Franck-Condon factor. Curve iii shows the fluorescence when only the rotational mixing microwaves are turned off between $14 - 19$ ms. The $1/e$ decay due to pumping into rotational dark states has a 7.4 ms time constant (inset curve iii). By combining the ratio of the two loss rates and q_{01}, we estimate the branching ratio from $A^2\Pi_{1/2}$ to $A'^2\Delta_{3/2}$ to be $\sim 3 \times 10^{-4}$. This branching ratio agrees with the value derived from transition dipole moments calculated in Ref. [39] and is similar to the combined branching ratio to $v'' \geq 2$. At 19 ms after ablation, the vibration repump (curve ii) and mixing microwaves (curve iii) are turned back on and the

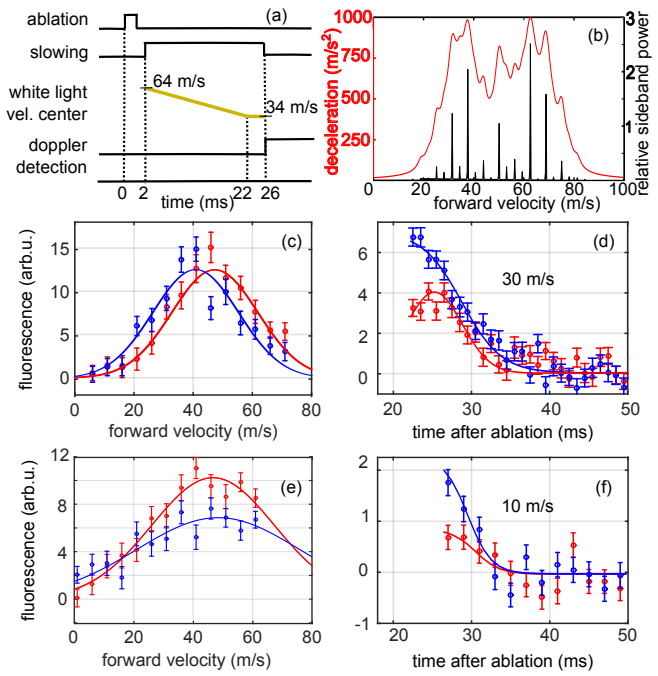

FIG. 4. (Color online) (a) Timing sequence used to slow molecules to below 10 m/s. (b) Example of spectrally broadened slowing light with center velocity of 50 m/s. Black lines show the sidebands generated from an EOM and rapid polarization switching. The red curve shows molecular deceleration with an optical saturation parameter of 3. (c-f) Comparisons between no slowing in red and with slowing in blue. Solid lines are guides to the eye. (c) Doppler spectra for a 10 ms long slowing sequence. (d) Time of flight for 30 m/s molecules. (e) Doppler spectra for a 24 ms long slowing sequence as depicted in (a). (f) Time of flight for 10 m/s molecules.

fluorescence immediately recovers.

We estimate the capture velocity of a 3D MOT for YO with a laser beam diameter of 1 cm to be 10 m/s. To slow some fraction of the molecules to below this capture velocity, we apply longitudinal radiation pressure slowing with protocols shown in Fig. 4(a). To increase the fraction of molecules addressed by the slowing beam, we spectrally broaden the light [42] via a resonant electro-optic modulator (EOM) with a modulation frequency of 10 MHz and a phase modulation index of 3.3. This spectrally broadens each laser frequency to ±30 MHz, corresponding to a velocity spread of ±20 m/s. Polarization switching used for destabilizing Zeeman dark states [27] further adds 5 MHz sidebands and we obtain frequency components spaced by the natural linewidth of the main cooling transition, ensuring continuous deceleration across this velocity range (Fig. 4(b)).

As the range of the slowing force is smaller than the velocity spread of the YO beam itself, we implement frequency chirping on the slowing light. In Fig. 4(c) and (d), the slowing sequence is designed to enhance molecules at 30 m/s. The molecules propagate freely for the first 12 ms after ablation, then the slowing beam is turned on from 12-22 ms. During this time, the center of the broadband radiation is linearly swept from being resonant with 64 m/s to 44 m/s molecules. In panel (c), we see a molecular population enhancement between $20-40$ m/s (negligible for below 20 m/s), and depletion for velocities greater than 40 m/s. In panel (d), we maintain the probe laser's frequency to be resonant with the 30 m/s molecule and observe an enhancement in the number of molecules in this velocity class. Due to off-resonant excitations, some faster molecules (35 m/s) contribute to the detected signal at 27 ms for the unslowed case.

To produce even slower molecules, we increase the time during which the slowing laser is turned on and perform a frequency chirp to address lower velocity molecules. The slowing light is turned on 2 ms after ablation and is left on for the next 24 ms. During the first 20 ms, the center frequency of the broadband slowing laser is linearly increased from being resonant with 64 m/s to 34 m/s molecules (Fig. 4(a)). Figure 4(e) shows the velocity distribution after the slowing sequence compared to the original velocity distribution. Slowing enhances the molecular population below 20 m/s and depletes molecules with velocities higher than 20 m/s. We tune the probe laser frequency to be resonant with the 10 m/s molecule and we see a clear enhancement in the number of molecules in this velocity class (Fig. 4(f)). Unslowed molecules leaving the cell with 10 m/s forward velocity will arrive 89 ms after the ablation, well after the detection time. Hence, we attribute the non-zero 10 m/s signal in the unslowed case to off-resonant excitations from fast molecules.

For the detection time windows shown in Fig. 4(d,f), we estimate the percentage of molecules in the 30 m/s and 10 m/s velocity classes with a Doppler resolution of ±3 m/s to be 2% and 0%, respectively for the unslowed beam, based on Fig. 2(c). The laser slowing enhances the corresponding population fractions to be 3% and 0.1% of the total original distribution. We note that without microwave mixing, the radiation pressure slowing stops working due to the fast optical pumping to the dark states.

We demonstrate enhanced optical cycling in YO via microwave mixing of rotational states in the ground electronic state. This enabled us to slow longitudinally the YO beam via radiation pressure, producing molecules that can be loaded into a 3D MOT. Because this technique maintains rotational closure with less stringent requirements on the cycling transition, it becomes relatively straightforward to perform laser cooling of molecules on $J'' \rightarrow J' = J'' + 1$ transitions, which would avoid the complications of dark states that are present in $J'' \rightarrow J' = J'' - 1$ molecular MOTs [27, 43], as was originally proposed [25]. This opens the door to laser cooling a greater variety of molecules with more choices of cooling transitions. To further close the vibrational

branching to $< 10^{-6}$, an additional $v' = 1 \leftarrow v'' = 2$ repump laser at 649 nm can be used [27, 37]. By turning off the microwave mixing for $N'' = 1 \leftrightarrow N'' = 0$ at an appropriate time, we can accumulate trapped cold YO in the ro-vibrational ground state. The $A'^2\Delta_{3/2}$ state lifetime of $\sim$1 μs opens up the possibility of a narrow line MOT [44, 45].

We thank M. Petzold and M. Kuhnert for their contributions to the early stage of this work. This work was supported in part by the Gordon and Betty Moore Foundation through Grant GBMF3852 to J.Y. We also acknowledge funding support from ARO (MURI), AFOSR (MURI), the NSF Physics Frontier Centers at both JILA and Harvard, and NIST.

* yeoe@jila.colorado.edu

[1] L. D. Carr, D. DeMille, R. V. Krems, and J. Ye, New. J. Phys. **11**, 055049 (2009).
[2] (The ACME Collaboration) J. Baron *et al.*, Science **343**, 269 (2014).
[3] J. J. Hudson, D. M. Kara, I. J. Smallman, B. E. Sauer, M. R. Tarbutt, and E. A. Hinds, Nature **473**, 493 (2011).
[4] L. R. Hunter, S. K. Peck, A. S. Greenspon, S. S. Alam, and D. DeMille, Phys. Rev. A **85**, 012511 (2012).
[5] X. Zhuang, A. Le, T. C. Steimle, N. E. Bulleid, I. J. Smallman, R. J. Hendricks, S. M. Skoff, J. J. Hudson, B. E. Sauer, E. A. Hinds, and M. R. Tarbutt, Phys. Chem. Chem. Phys. **13**, 19013 (2011).
[6] T. A. Isaev, S. Hoekstra, and R. Berger, Phys. Rev. A **82**, 052521 (2010).
[7] H. P. Büchler, E. Demler, M. Lukin, A. Micheli, N. Prokof'ev, G. Pupillo, and P. Zoller, Phys. Rev. Lett. **98**, 060404 (2007).
[8] N. Y. Yao, A. V. Gorshkov, C. R. Laumann, A. M. Läuchli, J. Ye, and M. D. Lukin, Phys. Rev. Lett. **110**, 185302 (2013).
[9] B. Yan, S. A. Moses, B. Gadway, J. P. Covey, K. R. A. Hazzard, A. M. Rey, D. S. Jin, and J. Ye, Nature **501**, 521 (2013).
[10] S. Ospelkaus, K.-K. Ni, D. Wang, M. H. G. de Miranda, B. Neyenhuis, G. Qumner, P. S. Julienne, J. L. Bohn, D. S. Jin, and J. Ye, Science **327**, 853 (2010).
[11] M. T. Bell and T. P. Softley, Mol. Phys. **107**, 99 (2009).
[12] B. C. Sawyer, B. K. Stuhl, M. Yeo, T. V. Tscherbul, M. T. Hummon, Y. Xia, J. Klos, D. Patterson, J. M. Doyle, and J. Ye, Phys. Chem. Chem. Phys. **13**, 19059 (2011).
[13] K. Ni, S. Ospelkaus, M. H. G. D. Miranda, A. Pe'er, B. Neyenhuis, J. J. Zirbel, S. Kotochigova, P. S. Julienne, D. S. Jin, and J. Ye, Science **322**, 231 (2008).
[14] D. R. Miller, *Atomic and Molecular Beam Methods*, edited by G. Scoles (Oxford University Press, 1988) p. 20.
[15] N. R. Hutzler, Hsin-I. Lu, and J. M. Doyle, Chem. Rev. **112**, 4803 (2012).
[16] Hsin-I Lu, I. Kozyryev, B. Hemmerling, J. Piskorski, and J. M. Doyle, Phys. Rev. Lett. **112**, 113006 (2014).
[17] S. Y. T. van de Meerakker, N. Vanhaecke, and G. Meijer, Annu. Rev. Phys. Chem. **57**, 159 (2006).
[18] B. C. Sawyer, B. K. Stuhl, D. Wang, M. Yeo, and J. Ye, Phys. Rev. Lett. **101**, 203203 (2008).
[19] E. Narevicius, A. Libson, C. G. Parthey, I. Chavez, J. Narevicius, U. Even, and M. G. Raizen, Phys. Rev. Lett. **100**, 093003 (2008).
[20] S. D. Hogan, A. W. Wiederkehr, H. Schmutz, and F. Merkt, Phys. Rev. Lett. **101**, 143001 (2008).
[21] B. K. Stuhl, M. T. Hummon, M. Yeo, G. Quéméner, J. L. Bohn, and J. Ye, Nature **492**, 396 (2012).
[22] S. Chervenkov, X. Wu, J. Bayerl, A. Rohlfes, T. Gantner, M. Zeppenfeld, and G. Rempe, Phys. Rev. Lett. **112**, 013001 (2014).
[23] M. Zeppenfeld, B. G. U. Englert, R. Glöckner, A. Prehn, M. Mielenz, C. Sommer, L. D. van Buuren, M. Motsch, and G. Rempe, Nature **491**, 570 (2012).
[24] M. Di Rosa, Eur. Phys. J. D. **31**, 395 (2004).
[25] B. K. Stuhl, B. C. Sawyer, D. Wang, and J. Ye, Phys. Rev. Lett. **101**, 243002 (2008).
[26] E. S. Shuman, J. F. Barry, and D. Demille, Nature **467**, 820 (2010).
[27] M. T. Hummon, M. Yeo, B. K. Stuhl, A. L. Collopy, Y. Xia, and J. Ye, Phys. Rev. Lett. **110**, 143001 (2013).
[28] J. F. Barry, D. J. McCarron, E. B. Norrgard, M. H. Steinecker, and D. DeMille, Nature **512**, 286 (2014).
[29] D. J. McCarron, E. B. Norrgard, M. H. Steinecker, and D. DeMille, arXiv:1412.8220.
[30] B. Hemmerling, G. K. Drayna, E. Chae, A. Ravi, and J. M. Doyle, New J. Phys. **16**, 063070 (2014).
[31] W. D. Phillips and H. Metcalf, Phys. Rev. Lett. **48**, 596 (1982).
[32] V. Zhelyazkova, A. Cournol, T. E. Wall, A. Matsushima, J. J. Hudson, E. A. Hinds, M. R. Tarbutt, and B. E. Sauer, Phys. Rev. A **89**, 053416 (2014).
[33] N. Vanhaecke and O. Dulieu, Mol. Phys. **105**, 1723 (2007).
[34] M. Kirste, X. Wang, G. Meijer, K. B. Gubbels, A. van der Avoird, G. C. Groenenboom, and S. Y. T. van de Meerakker, J. Chem. Phys. **137**, 101102 (2012).
[35] C. L. Chalek and J. L. Gole, J. Chem. Phys. **65**, 2845 (1976).
[36] A. R. Allouche, G. Wannous, and M. Aubert-Frécon, Chem. Phys. **170**, 11 (1993).
[37] A. Bernard and R. Gravina, Astrophys. J. Suppl. Ser. **52**, 443 (1983).
[38] E. S. Shuman, J. F. Barry, D. R. Glenn, and D. DeMille, Phys. Rev. Lett. **103**, 223001 (2009).
[39] S. R. Langhoff, and C. W. Bauschlicher, J. Chem. Phys. **89**, 2160 (1988).
[40] W. J. Childs, O. Poulsen, and T. C. Steimle, J. Chem. Phys. **88**, 598 (1988).
[41] J. M. Brown and A. Carrington, *Rotational Spectroscopy of Diatomic Molecules* (Cambridge University Press, 2003).
[42] M. Zhu, C. W. Oates, and J. L. Hall, Phys. Rev. Lett. **67**, 46 (1991).
[43] M. R. Tarbutt, New J. Phys. **17**, 015007 (2015).
[44] T. H. Loftus, T. Ido, A. D. Ludlow, M. M. Boyd, and J. Ye, Phys. Rev. Lett. **93**, 073003 (2004).
[45] A. L. Collopy, M. H. Hummon, M. Yeo, B. Yan, and J. Ye, "Prospects for a narrow line MOT in YO," arXiv:1501.05326.